

available at www.sciencedirect.comjournal homepage: www.elsevier.com/locate/biochempharm

Nuclear translocation of telomerase reverse transcriptase and calcium signaling in repression of telomerase activity in human lung cancer cells by fungal immunomodulatory protein from *Ganoderma tsugae*

Chien-Huang Liao^a, Yi-Min Hsiao^b, Gwo-Tarng Sheu^a, Jinghua Tsai Chang^a,
Po-Hui Wang^d, Ming-Fang Wu^e, Gow-Jen Shieh^f, Chung-Ping Hsu^{c,*}, Jiunn-Liang Ko^{a,*}

^a Institute of Medical and Molecular Toxicology, Chung Shan Medical University, Taichung, Taiwan, ROC

^b Institute of Medical Biotechnology, Central Taiwan University of Science and Technology, Taichung, Taiwan, ROC

^c Department of Thoracic Surgery, Veterans General Hospital-Taichung, Taichung, Taiwan, ROC

^d Department of Obstetrics and Gynecology, Chung Shan Medical University Hospital, Taichung, Taiwan, ROC

^e Department of Medical Oncology and Chest Medicine, Chung Shan Medical University Hospital, Taichung, Taiwan, ROC

^f National Taiwan University Hospital Yun-Lin Branch, Taiwan, ROC

ARTICLE INFO

Article history:

Received 11 May 2007

Accepted 18 July 2007

Keywords:

Fungal immunomodulatory protein

ER stress

hTERT

Nuclear export

ABSTRACT

Recombinant fungal immunomodulatory protein, reFIP-gts, was cloned from *Ganoderma tsugae* and purified. In our previous study, it was shown that reFIP-gts has anti-telomerase effects in A549 cells. Here, we proved that reFIP-gts entry into the cell and localization in endoplasmic reticulum can result in ER stress, thereby increasing ER stress markers (CHOP/GADD153) and intracellular calcium release in A549 cells. The use of calcium chelator restores reFIP-gts-mediated reduction in telomerase activity. These results strongly suggest that ER stress induces intracellular calcium release and results in inhibition of telomerase activity. Although reFIP-gts decreased hTERT mRNA level in both A549 and H1299 cells, only the telomerase activity in A549 cells was inhibited. Surprisingly, we found that reFIP-gts induces translocation of hTERT from the nucleus into the cytosol in A549 cells but not in H1299 cells. Using leptomycin B, nuclear export inhibitor, we showed that hTERT is not transported. Using MG132, a proteasome inhibitor, reFIP-gts also prevents hTERT translocation from proteasome degradation. Taken together, these results indicate that reFIP-gts inhibits telomerase activity in lung cancer cells through nuclear export mechanisms, which might be mediated by ER stress-induced intracellular calcium level.

© 2007 Elsevier Inc. All rights reserved.

* Corresponding authors at: Institute of Medical and Molecular Toxicology, Chung Shan Medical University, 110, Sec. 1, Chien-Kuo N. Road, Taichung, Taiwan 40203, ROC. Tel.: +886 4 24730022 11694; fax: +886 4 24751101.

E-mail addresses: cliff@vghc.vghc.gov.tw (C.-P. Hsu), jlko@csmu.edu.tw (J.-L. Ko).

Abbreviations: reFIP-gts, recombinant fungal immunomodulatory protein *Ganoderma tsugae*; hTERT, human telomerase reverse transcriptase; ER, endoplasmic reticulum; GADD153, growth arrest- and DNA damage-inducible gene 153; TG, thapsigargin 0006-2952/\$ – see front matter © 2007 Elsevier Inc. All rights reserved.

doi:10.1016/j.bcp.2007.07.025

1. Introduction

Telomerase is a cellular reverse transcriptase that catalyzes the synthesis and extension of telomeric DNA. In the absence of telomerase, telomeres shorten as cells divide until senescence [1]. Telomerase activity is undetectable in normal somatic cells. However, the length of telomere is stabilized and telomerase activity can be detected in about 85% of cancer cells. Reactivation of telomerase is believed to be involved in cellular immortalization and tumorigenesis [2]. In our previous study, we found that loss of telomerase activity may be a potentially favorable prognostic marker in lung carcinomas [3]. Therefore, telomerase has been proposed to represent a marker for carcinogenesis and potentially a selective target for cancer therapy.

The telomerase complex is composed of telomerase reverse transcriptase (TERT), which functions as the catalytic subunit of telomerase [4] and telomerase RNA (TR), and as a template for telomere elongation. Expression of hTERT correlates with telomerase activity during cellular differentiation and neoplastic transformation in a variety of cancers [5–7], suggesting that hTERT may be transcriptionally regulated [8]. Multiple mechanisms may regulate hTERT expression and activity. Transcription factors, for example, are involved in the up-regulation or down-regulation of hTERT transcriptional activity [9,10], and the transactivator of hTERT, c-Myc, has received much attention.

In addition to transcriptional regulation, hTERT activity might be regulated by posttranslational modifications. Akt and protein kinase C (PKC), for example, contribute to the post-transcriptional regulation of the enzyme activity by kinase phosphorylation [11,12]. Another possible mechanism for posttranslational modulation of telomerase activity is through the interaction between hTERT and accessory proteins. For example, 14-3-3 proteins and nuclear factor- κ B (NF- κ B) possibly act as posttranslational modifiers of telomerase by controlling the intracellular localization of hTERT [13,14]. Some studies have found that expression of hTERT is very stable, with no significant changes in hTERT protein expression profile, when keratinocyte is treated with thapsigargin for a period of 6 days [15,16]. The 26 S proteasome is a primary constituent of the protein degradation apparatus of the cell and is responsible for the elimination of >80% of all cellular proteins. For instance, the up-regulation of telomerase activity in human T lymphocytes has been associated with the phosphorylation of hTERT protein and its nuclear translocation [17]. Changes in subcellular location of hTERT can activate telomerase through phosphorylation of hTERT and its translocation to the nucleus.

A group of fungal immunomodulatory proteins (FIPs) has been isolated and purified from *Ganoderma tsugae* (FIP-gts). These proteins are mitogenic in human peripheral blood lymphocytes (hPBLs) and mouse splenocytes. Activation of hPBLs with FIPs results in the increased production of the molecules IL-2 and IFN- γ and tumor necrosis factor- α associated with ICAM-1 expression [18,19]. FIPs may also have anticancer effects. Our previous study found that reFIP-gts significantly and selectively inhibits the growth of A549 cancer cells but does not affect normal MRC-5 fibroblasts. reFIP-gts has also been found to suppress telomerase activity

and to inhibit the transcriptional regulation of hTERT through a c-Myc-responsive element-dependent mechanism [20].

ER stress is induced when excess wild-type or misfolded proteins from extra-cellular endocytosis or intra-cellular production accumulate in the ER [21]. The ER serves several important functions, including post-translational modification, folding and assembly of newly synthesized proteins, and regulated calcium storage [22]. When ER is stimulated by agents, such as thapsigargin, that inhibit the Ca²⁺-ATPase, it stores large amounts of Ca²⁺ which are released into the cytoplasm [23,24]. Calcium might be a key regulator in this process. Calcium-induced differentiation has been associated with inhibition of telomerase activity in keratinocytes [16,25], and ingested calcium has been reported to induce telomerase activity in ovarian epithelial cells through c-jun NH2-terminal kinase (JNK) and proline-rich tyrosine kinase-dependent pathway (Pyk2) [26].

We hypothesized that reFIP-gts diffuses in ER, causing ER to release calcium into cytosol where alteration of the telomerase inhibits telomerase activity. Using immunocytochemical staining to observe translocation of hTERT and using fluor-3AM to detect levels of calcium, we found that ER is a target for reFIP-gts and decreased telomerase activity may be mediated by calcium-derived ER stress.

2. Materials and methods

2.1. Cell lines and chemicals

We obtained A549 human lung adenocarcinoma cells and H1299 human NSCLC cells from the American Type Culture Collection. Both cell lines were maintained at 37 °C in a 5% CO₂ humidified atmosphere in Dulbecco's modified Eagle's medium (DMEM)(GIBCO, Rockville, MD) containing 10% fetal bovine serum (FBS; Life Technologies, Inc., Rockville, MD) and 100 ng/ml each of penicillin and streptomycin (Life Technologies, Inc.). A549-p53 RNAi stable cell line was kindly provided by Dr. J.T. Chang (CSMU, Institute of Medical and Molecular Toxicology, Taichung, Taiwan). H1299-p53 stable cell line was developed as previously described [27]. Thapsigargin, cycloheximide, 1,2-bis (2-aminophenoxy) ethane N,N,N',N'-tetraacetic acid (BAPTA-AM) and Z-Leu-Leu-al (MG132) were obtained from Sigma (St. Louis, MO, USA). Furo-3 AM and pluronic acid F-127 were purchased from Molecular Probes (Eugene, OR, USA). Leptomycin B (L-6100) was obtained from LC Laboratories (Woburn, MA, USA).

2.2. Assay for telomerase activity

Telomerase activity was measured using the modified telomere repeat amplification protocol (TRAP) assay. Briefly, pelleted cells were lysed with 100 μ l of 1X CHAPS lysis buffer (10 mM Tris-HCl [pH 7.5], 1 mM EGTA, 0.5% CHAPS, 10% [v/v] glycerol, 5 mM β -2-mercaptoethanol and 0.1 mM phenylmethylsulfonyl fluoride), incubated on ice for 30 min and centrifuged for 30 min at 4 °C (13,000 \times g). The concentration of protein in the supernatant extracts was measured using BSA Protein Assay Kit (Pierce, IL, USA). TRAP assay was performed as previously described [20], with only minor

modifications, using a set of primers (TS, 5'-AATCCGTCGAG-CAGAGTT-3'; ACX, 5'-GCGCGGCTTACCCCTTAC CTTACCC-TAAC-3'); and an internal standard, NT, 5'-ATCGCTTC-TCGGCCTTTT-3' and TSNT (5'-AATCCGTCGAGCAGAGT-TAAAAGGCCGAGAAGCGAT-3'). Reaction mixtures were incubated at 25 °C for 30 min for telomerase-mediated extension and the samples were heated to 85 °C for 10 min. Taq polymerase was added and each sample was amplified for 30 cycles of polymerase chain reaction (PCR) amplification (94 °C for 30 s, 59 °C for 30 s and 72 °C for 90 s) in a DNA thermal cycler (GeneAmp PCR System 2400, PerkinElmer Co., Norwalk, CT, USA). TRAP products were resolved by 12.5% (w/v) non-denaturing polyacrylamide gel electrophoresis (PAGE) and visualized by staining with ethidium bromide. Activity of each sample was normalized to that of 50 ng of total cellular protein. Signal intensity in each lane was determined by measuring the area occupied by the first 6 ladders from the bottom of the gel using MultiImage™ (Alpha Innotech Corporation). Relative telomerase activities were quantified by comparing the signal intensities of the lanes with those of the positive controls (extract of untreated cells), with an intensity of 100% considered the standard.

2.3. Isolation of RNA and RT-PCR

Total cellular RNA was extracted from cells using the guanidium thiocyanate method [18]. Then, cDNA was reverse-transcribed from 1 µg total cellular RNA using random hexamer primers and murine leukemia virus reverse transcriptase. The primer sequences used for PCR amplification were: GADD153 sense 5'-GCCTTCTCTTCGGACACTG-3' and antisense 5'-TCAC-CATTCGGTCAATCAGA-3' [28]; hTERT sense 5'-AGTTCCT-GCACTGGCTGATG AGT3' and antisense 5'-CTCGGCCCTCTT-TCTCTGCG-3' [20]. One microliter of cDNA (100 ng) was amplified in a reaction volume of 50 µl containing 0.5 units of Taq polymerase (Ex taq, TaKaRa), 200 mM dNTPS, 10 mM Tris-HCl (pH8.0), 1.5 mM MgCl₂, 75 mM KCl and 20 pmol of each primer. The PCR reaction involved denaturation (94 °C, 5 min) followed by 35 cycles for GADD153, each consisting of denaturation (94 °C, 1 min), annealing (55 °C, 1 min) and extension (72 °C, 2 min) with a final extension phase (10 min). The PCR reaction was performed on a programmable thermal controller instrument-thermal cycler Model 2400.

Meanwhile, the same amount of cDNA was amplified using specific β-actin including sense and antisense primers (CAGGGAGTGATGGTGGGCA, CAAACATCATCTGGT CATCTT-CTC), according to the manufacturer's instructions (Life Technologies). The samples underwent 1 cycle of 5 min at 94 °C followed by denaturation (94 °C, 1 min), annealing (60 °C, 1 min) and extension (72 °C, 2 min), and an additional 27 cycles. The final cycle was modified to allow for a 10-min extension at 72 °C. The products were visualized using electrophoresis on 1.5% agarose gel and stained with ethidium bromide. We confirmed the quality of cellular mRNA by measuring the intensity of β-actin.

2.4. Chromatin immunoprecipitation (CHIP) analysis

To analyze chromatin immunoprecipitation, we modified a method described in a previous report [29]. Following treat-

ments for 24 h at various concentrations of reFIP-gts, approximately 2×10^7 adherent A549 cells were cross-linked for 15 min at 25 °C by adding 11% formaldehyde stock (50 mM HEPES-KOH at pH 8; 1 mM EDTA; 0.5 mM EGTA; 100 mM NaCl; 11% formaldehyde) to a final concentration of 1% formaldehyde for 15 min. Cross-linking was stopped by adding glycine to a final concentration of 125 mM for 5 min. The cell monolayers were rinsed with ice cold phosphate buffered saline, scraped into 50-ml conical tubes, and centrifuged at $600 \times g$ for 5 min at 4 °C. Pellets were aspirated and resuspended in 10 ml lysis buffer (50 mM HEPES-KOH at pH 8; 1 mM EDTA; 0.5 mM EGTA; 140 mM NaCl; 10% glycerol; 0.5% NP-40; 0.25% Triton X-100; 1 mM PMSF; 5 µg/ml each of leupeptin, pepstatin A, and aprotinin) and incubated for 10 min at 4 °C. The crude nuclei were collected by centrifugation ($600 \times g$ for 5 min at 4 °C), resuspended in 10 ml wash buffer (10 mM Tris-HCl at pH 8; 1 mM EDTA; 0.5 mM EGTA; 200 mM NaCl; 1 mM PMSF; 5 µg/ml each of leupeptin, pepstatin A, and aprotinin) and incubated again. Washed nuclei were centrifuged as described earlier and resuspended in 2 ml of 1× RIPA Buffer (10 mM Tris-HCl at pH 8; 1 mM EDTA; 0.5 mM EGTA; 140 mM NaCl; 1% Triton X-100; 0.1% Na-deoxycholate; 0.1% SDS; 1 mM PMSF; 5 µg/ml each of leupeptin, pepstatin A, and aprotinin). Samples were sonicated (power setting 5) with a Branson Sonifier 250 with a microtip in 20-s bursts followed by 1 min of cooling on ice for a total sonication time of 3 min per sample. This procedure resulted in DNA fragment sizes of 0.3–1.5 kb. Samples were then centrifuged in an Eppendorf 5415C centrifuge at $16,000 \times g$ for 10 min at 4 °C. To 600-µl aliquots of cleared chromatin extract, 2 µg of anti-c-Myc (Santa Cruz Biotechnology) antibodies were added. The mixture was incubated with rotation at 4 °C for 18 h with 20 µl of precleared 50% slurry Protein A/G beads (Zymed) in 1× RIPA Buffer containing 100 µg/ml sonicated salmon sperm DNA. After bead rotating, samples were centrifuged at $600 \times g$ and the pellets were washed twice with 1× RIPA buffer, once with 1× RIPA buffer containing 100 µg/ml salmon sperm DNA for 5 min with rotation, five times with 1× RIPA buffer containing 500 mM NaCl final plus 100 µg/ml salmon sperm DNA for 5 min with rotation, and once again with 1× RIPA buffer. Then, 100 µl of digestion buffer were added (50 mM Tris at pH 8; 1 mM EDTA; 100 mM NaCl; 0.5% SDS; 100 µg/ml proteinase K) for 6 h at 65 °C to reverse cross-links. DNA was phenol-CHCl₃ extracted once, CHCl₃ extracted once, and ethanol precipitated in the presence of 20 µg glycogen. Pellets were resuspended in 20 µl TE, and used for PCR amplification of the hTERT gene promoter DNA. The primers for hTERT PCR were 5'-CGCGCTTCC CACGTGGCGGAGGGA -3' and 5'-CCCACGTGCGCAGCAGGACGC A-3' for a 254-bp TERT promoter DNA. Normal IgG was used as a negative control.

2.5. Intracellular free calcium measurements

Cells were grown on poly-L-lysine-coated glass coverslips at 5×10^4 cells in 35 mm dish, and then treated with 1.2 µM reFIP-gts for 6, 12 and 24 h or with 2.5 µM Thapsigargin for 6 and 24 h. Other cells were pretreated with 20 µM BAPTA-AM for 1 h and then treated with 1.2 µM reFIP-gts for 24 h. Cells were rinsed twice with Hank's buffered salt solution (HBSS) (20 mM HEPES, 10 mM glucose, 150 mM NaCl, 1.2 mM CaCl₂,

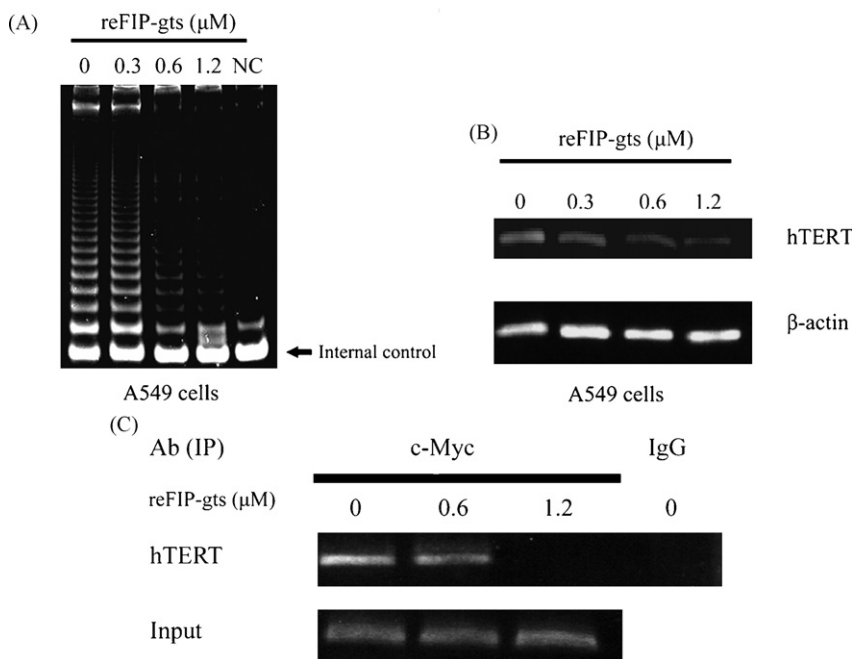


Fig. 1 – Effect of reFIP-gts on telomerase activity and hTERT expression in A549 cells. (A) Effect of reFIP-gts on the level of telomerase activity in A549 cells. Twenty-four hours after plating, cells were exposed to various concentrations of reFIP-gts (0, 0.3, 0.6 and 1.2 μM) for 48 h. Cell pellets were collected and subjected to TRAP assay. NC, negative control used lysis buffer only. Internal control, the 36-bp internal standard was used as control. (B) Total cellular RNA from A549 cells, untreated or treated with 0.3, 0.6 and 1.2 μM reFIP-gts for 12 h, analyzed using RT-PCR for hTERT and β-actin for mRNA expression. Representative photograph from an experiment repeated three times. (C) ChIP assay was performed on reFIP-gts-treated A549 cells (0, 0.6 and 1.2 μM) for 24 h, and the precipitated chromatin was PCR-amplified with the use of specific primers with E-boxes in the hTERT promoter. In vivo identification of reciprocal E-box occupancy by c-Myc at the hTERT promoter in A549 cells was carried out. IgG antibodies were used as negative control. Input: PCRs performed on total chromatin from A549 cells.

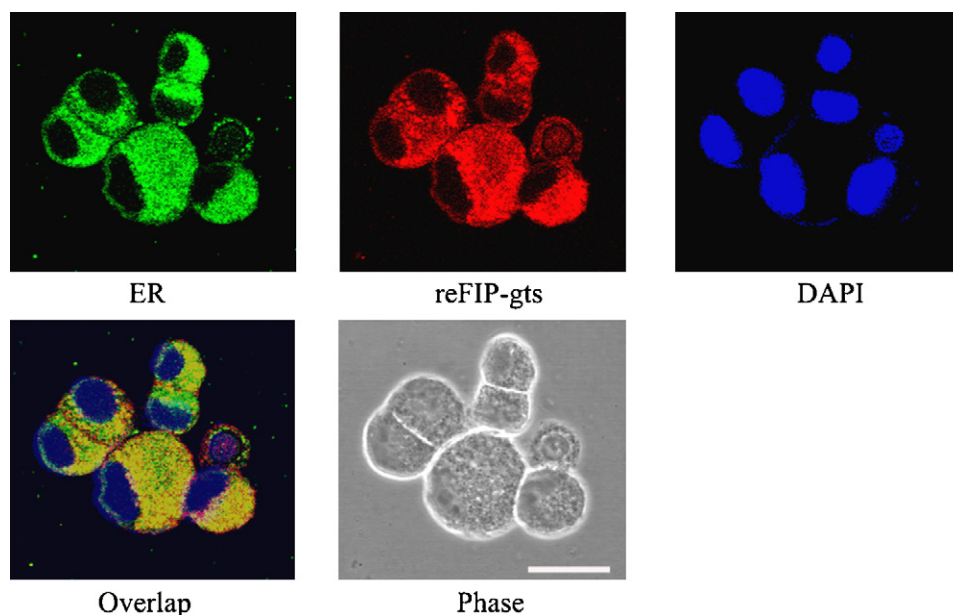


Fig. 2 – Subcellular localization of reFIP-gts in A549 cells. A549 cells treated with 1.2 μM reFIP-gts for 24 h. Cells were fixed, permeabilized and labeled with anti-reFIP-gts mAb (Rhodamine-Red), ER dye (FITC-Green) and DAPI stain (DAPI-Blue). The localization or colocalization (yellow) was detected by confocal microscopy scanning laser microscope (Leica TCS, 630×). Scale bar indicates 20 μm. (For interpretation of the references to colour in this figure legend, the reader is referred to the web version of the article.)

5 mM KCl, 1 mM MgCl_2 , pH 7.4). They were then loaded with 3 μM Fura-3 AM dissolved in HBSS from a working solution and 0.02% pluronic acid F-127 at 37 °C for 60 min and rinsed twice with HBSS. Next, the cells were incubated in HBSS for an additional 30 min to allow complete de-esterification of the dye. Calcium imaging was accomplished using an LSM 410 invert confocal laser scanning microscope (Carl Zeiss Jena, Germany). Excitation was done by the 488 nm line of an Ar laser. Emission 505–550 band pass filter was collected, and pinhole was set at 1.87 airy units. Confocal imaging was performed with a resolution of 512×512 pixel at 256 intensity. The frame rate was 1 frame/min. Several cells were viewed together through 20 \times Plan-Neofluar Zeiss (0.5 NA) using a factor-2 computer zoomed image. Detailed images were also collected using 40 \times Plan-Neofluar Zeiss (1.3 NA). Fluo-3 fluorescence was analyzed using Image J software (NIH). The data are presented as mean \pm standard deviation of triplicate experiments. The symbol (*) indicates $P < 0.05$ when compared with untreated

cells on Student's *t* test. SPSS 10.0 software (SPSS Inc., Chicago, IL) was used to perform statistical analyses.

2.6. Western blot analysis

Cells were lysed and protein concentration was assayed using Bio-Rad Protein Assay Kit (Bio-Rad, Hercules, CA, USA). Equal amounts of proteins were subjected to sodium dodecyl sulfate 10% polyacrylamide gel electrophoresis. Fractionated proteins were transferred to Hybond-P membrane. Membranes were blocked in PBS containing 5% nonfat milk and 0.2% Tween 20. To detect p53 and β -actin, monoclonal anti-p53 (Dako Corporation, Carpinteria, CA) (1:500) and monoclonal anti β -actin (AC-40, Sigma, St. Louis, MI, USA) were used. To detect hTERT and GADD153, polyclonal antibodies to hTERT (ROCKLAND, Gilbertsville, PA; dilution 1:500)[30] and GADD153 (LAB VISION, Fremont CA, USA) were used. To detect phospho-Akt and total Akt, polyclonal anti-phospho-Akt and total Akt (Cell

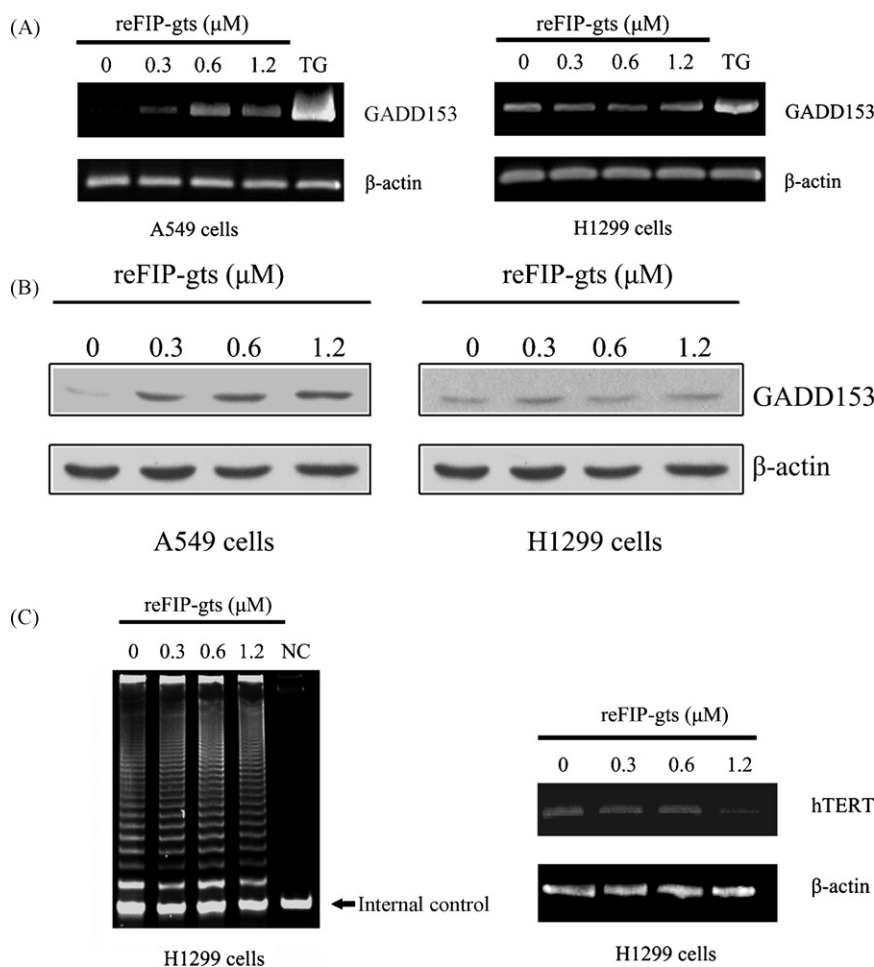


Fig. 3 – FIP-gts induces ER stress in A549 cells but not in H1299 cells. (A) A549 cells and H1299 cells were treated with varying concentrations (0, 0.3, 0.6 and 1.2 μM) of reFIP-gts or 2.5 μM thapsigargin (TG) for 48 h followed by RNA isolation and RT-PCR analysis as described in Section 2. (B) A549 cells and H1299 cells were treated with varying concentrations (0, 0.3, 0.6 and 1.2 μM) of reFIP-gts for 48 h followed by Western blot as described in Section 2. (C) Left part, effect of reFIP-gts on the level of telomerase activity in H1299 cells. Twenty-four hours after plating, cells were exposed to various concentrations of reFIP-gts (0, 0.3, 0.6 and 1.2 μM) for 48 h. Cell pellets were collected and subjected to TRAP assay. NC, negative control used lysis buffer only. Internal control, the 36-bp internal standard was used as control. Right part, total cellular RNA from H1299 cells untreated or treated with 0.3, 0.6 and 1.2 μM reFIP-gts for 12 h, with analysis using RT-PCR for hTERT and β -actin mRNA expression. Representative photograph from an experiment repeated three times.

Signaling Technology, Beverly, MA, USA; dilution 1:1000) were incubated with the membranes overnight at 4 °C, followed by anti-mouse or anti-rabbit IgG HRP-linked antibody horse-radish peroxidase-conjugated secondary antibody (Cell Signaling Technology, Beverly, MA, USA) for 1 h at RT. Blots were then developed using an enhanced luminol chemiluminescence (ECL) reagent (NEN, Boston, USA).

2.7. Fluorescence immunocytochemistry and confocal microscopy

A549 cells were seeded (1×10^4 cells per chamber) onto an eight-chamber slide (Nunc 177402, Naperville, IL). They were fixed in 4% paraformaldehyde for 20 min and permeabilized with 0.3% Triton X-100 in PBS for 20 min. Washed cells were incubated in 1% bovine serum albumin in PBS for 1 h. For co-immunostaining, cells were first incubated with an antibody against hTERT (rabbit, 1:250; 1 h, RT; Calbiochem, San Diego, CA). Tetramethyl rhodamine isothiocyanate goat anti-rabbit IgG (H + L) conjugate was used as a secondary antibody (1:100, 1 h; ZyMax™ Grade, Invitrogen, Carlsbad, CA). Slides were mounted with mount medium and dried at room temperature. Nuclei were counterstained with 0.2 µg of DAPI (4',6-diamidino-2-phenylindole)/ml. Computer-assisted image analysis

of fluorescence was performed using confocal microscopy scanning laser microscope (Leica TCS, wavelength excitation 488 nm, emission 525 nm for FITC; 540/570 nm for TRITC).

For the reFIP-gts and endoplasmic reticulum (ER) colocalization studies, the protocol was similar to that described above, except that after permeabilization cells were washed and incubated in 1% bovine serum albumin in PBS for 1 h and then incubated with an antibody against reFIP-gts (mouse, 1:500; 1 h, RT). Tetramethyl rhodamine isothiocyanate goat mouse conjugate was used as a secondary antibody (1:100, 1 h; ZyMax™ Grade, Invitrogen, Invitrogen, Carlsbad, CA). For ER staining, cells were incubated with ER stain solution at 37 °C for 45 min (1:3000; Subcellular Structure Localization Kit, Chemicon, Temecula, CA), then mounted and visualized by confocal microscopy.

3. Results

3.1. Recombinant FIP-gts suppresses telomerase activity via repression of c-myc binding

Our previous studies have shown that reFIP-gts significantly inhibits telomerase activity and the interaction between E-box

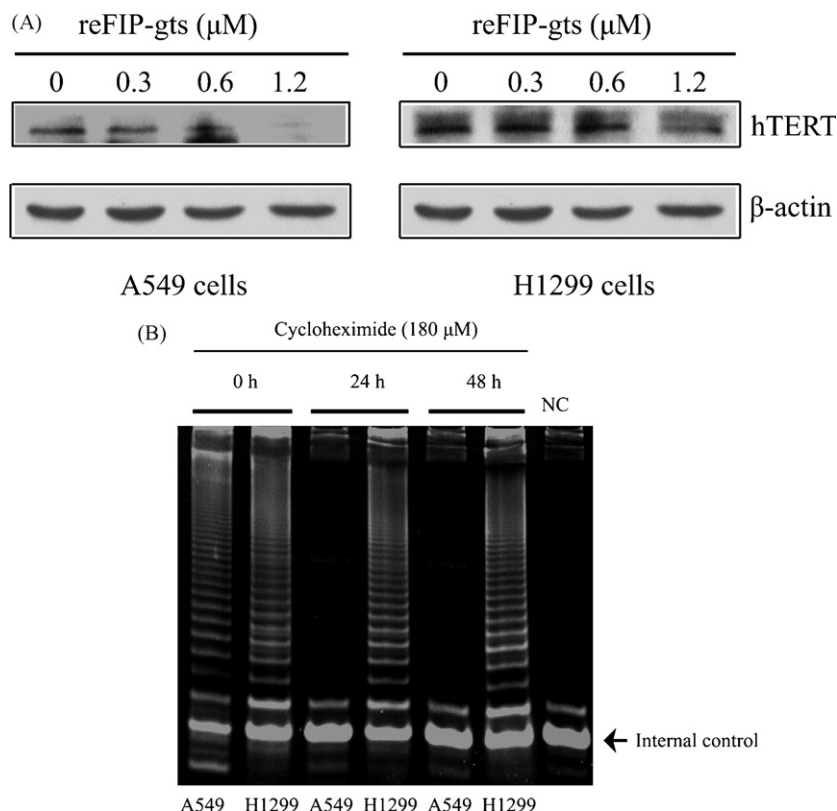


Fig. 4 – (A) Effect of reFIP-gts on hTERT expression in A549 and H1299 cells. A549 and H1299 cells were untreated or treated with 0, 0.3, 0.6 and 1.2 µM reFIP-gts for 48 h, and Western blotting analysis of the cell lysates was performed to detect hTERT expression. The protein β-actin was used as an internal control for normalization of protein loading. **(B)** Half-life of telomerase activity in cycloheximide-treated cells. A549 and H1299 cells were treated with a final concentration of 180 µM of Cycloheximide per ml for 48 h. Cells were harvested at the indicated times and tested for telomerase activity by TRAP assay. The subsequent levels of telomerase activity are represented as a fraction of the 0-h activity. IC: the 36-bp internal standard was used as internal control. The data are representative of three independent experiments. NC: no telomerase extract was added.

region of the hTERT promoter and c-Myc/Max transcription factor in A549 cells [20]. To determine whether reFIP-gts inhibits c-Myc binding to the endogenous hTERT gene in cultured A549 cells, we performed ChIP analysis using specific anti-c-Myc polyclonal antibody. Negative control for antibody was normal IgG. As shown in Fig. 1, reFIP-gts inhibited telomerase activity via transcriptional regulation of hTERT (Fig. 1A and B) and repressed c-Myc binding to endogenous hTERT promoter in A549 cells (Fig. 1C), a finding that was consistent with previous data using electrophoretic mobility shift assay.

3.2. Localization of recombinant FIP-gts in the endoplasmic reticulum

The molecular mechanism of the effects of reFIP-gts on telomerase activity is still unclear. The first step toward understanding the possible roles of reFIP-gts is to determine its cellular localization. Colocalization studies were performed using specific markers for the cellular organs and reFIP-gts in A549 cells. reFIP-gts was not located in the nucleus, and the markers of mitochondria and reFIP-gts did not overlap (data not shown). As shown in Fig. 2, on immunofluorescence the markers of reFIP-gts and ER overlapped, indicating that reFIP-gts had diffused into ER, and confirming that reFIP-gts targets ER.

3.3. Recombinant FIP-gts induction of endoplasmic reticulum stress

In a previous study, accumulation of proteins in ER was found to induce ER stress. We next examined whether reFIP-gts

triggers ER stress as it accumulates in the ER, by determining the effects of reFIP-gts on the expression of classical ER stress markers [31]. In these experiments, the ER Ca^{2+} -ATPase inhibitor thapsigargin served as a positive control for ER stress. RT-PCR and Western blotting analyses confirmed that, like thapsigargin, reFIP-gts induced CHOP/GADD153 mRNA and protein levels in A549 cells at 0.6 and 1.2 μM (Fig. 3A, left panel and B, left panel).

We investigated whether reFIP-gts induces ER stress in another lung cancer cell line, H1299 NSCLC. On RT-PCR and Western blotting analyses, reFIP-gts was unable to increase CHOP/GADD153 mRNA or protein levels in H1299 cells (Fig. 3A right panel and B right panel). We next examined the effects of reFIP-gts on telomerase activity in H1299 cells. On TRAP assay telomerase activity was not inhibited in H1299 cells (Fig. 3C, left panel). As shown in Fig. 3, 0.6 μM reFIP-gts more effectively induced GADD153 in A549 cells than 1.2 μM reFIP-gts, leading us to believe that reFIP-gts dose inhibition followed a bell-shaped curve for GADD153 in A549 cells. Interestingly, despite no reduction in telomerase activity in H1299 cells treated with reFIP-gts, mRNA level of hTERT was reduced significantly following treatment with 0.6 and 1.2 μM reFIP-gts, producing an effect similar to that in A549 cells (Fig. 3C, right panel). These results suggest a relationship between inhibition of telomerase activity and ER stress induction by reFIP-gts in A549 cells.

We further studied the effect of reFIP-gts on hTERT protein in A549 and H1299 cells, and confirmed our findings with Western blot. As shown in Fig. 4A, the protein level of hTERT was clearly reduced following 0.6 and 1.2 μM reFIP-gts

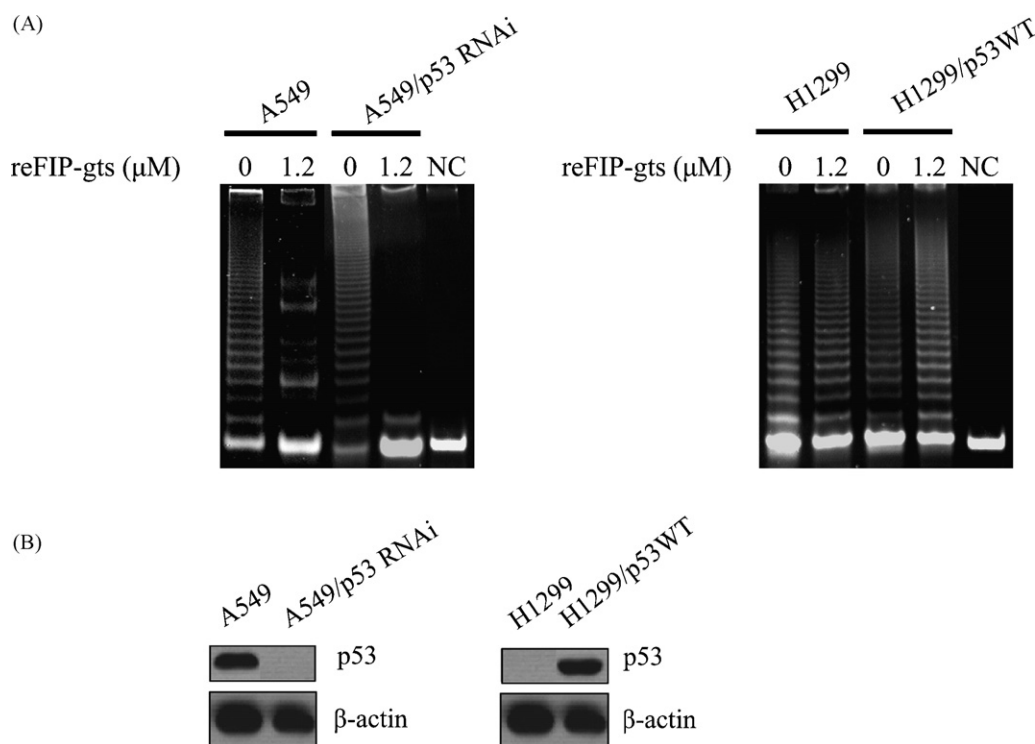
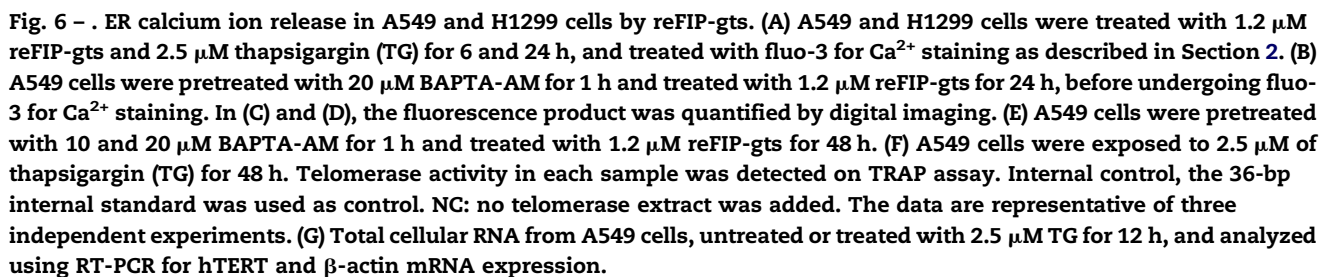


Fig. 5 – Tumor repressor p53 is not required in vivo to limit telomerase expression by reFIP-gts. (A) A549 cells (left) and H1299 cells (right) with or without p53 depletion or in two isogenic cell lines in the presence or absence of 1.2 μM reFIP-gts for 48 h. Cell pellets were collected and subjected to TRAP assay. **(B)** Immunoblotting was used to view the presence or absence of p53 in A549 cells (left) and H1299 cells (right).



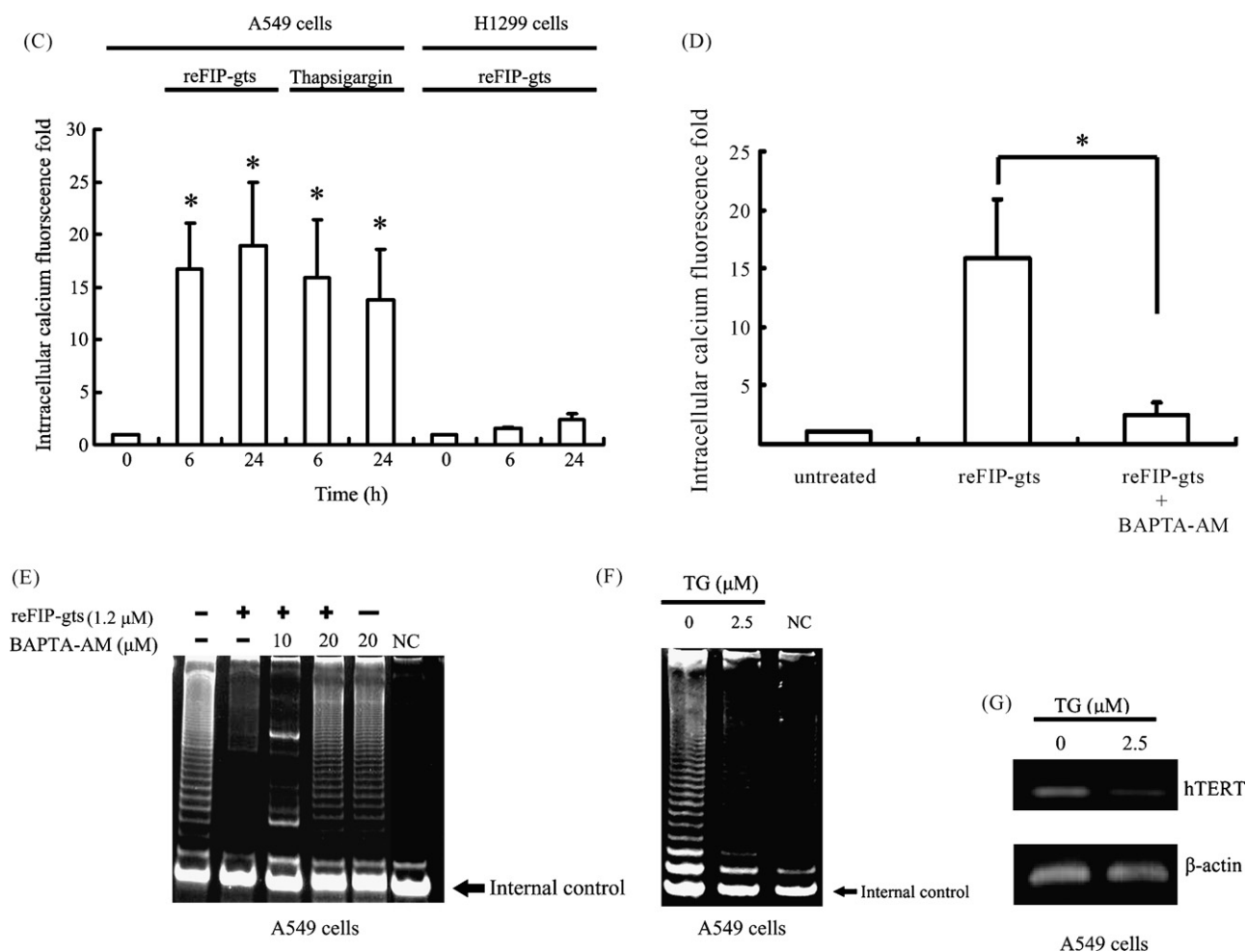


Fig. 6. (Continued).

treatment in A549 cells. However, the protein level of hTERT was only slightly reduced following 1.2 μM reFIP-gts treatment in H1299 cells.

Several studies have reported telomerase to be a highly stable protein complex with a long half-life [15,16]. The half-life of telomerase activity was determined in H1299 and A549 cells treated with cycloheximide, a potent inhibitor of protein synthesis. Using TRAP assay, we observed that telomerase activity decreased to <10% of the control level after 48 h in A549 cells, but this effect was not seen in H1299 cells (Fig. 4B). This finding suggests that the long half-life of telomerase in H1299 makes hTERT protein more stable in cell nucleus, notwithstanding the lack of expression of hTERT mRNA (Fig. 3C).

3.4. Independence of P53 on recombinant FIP-gts-regulated telomerase activity

Several studies have suggested that p53 is a negative regulator of hTERT [12,32], while other studies have shown that telomerase expression in tumors does not correlate with p53 status [9,33]. We found telomerase activity to be inhibited in A549 cells (wild-type p53), but not in H1299 cells (null p53). There are two possible explanations for the differences in

reFIP-gts-regulated telomerase activity between A549 and H1299. First, regulation of telomerase activity by reFIP-gts may be mediated by P53. Second, there are fundamental differences between the two cell lines including in uptake of reFIP-gts, intracellular localization of reFIP-gts, and other cellular components that mediate the effect of reFIP-gts. If p53 is a bona fide repressor of telomerase, then removal or overexpression of p53 should be able to modify the expression of telomerase. We depleted p53 using siRNA in A549 cells, and stably overexpressed p53 in H1299 cells. When p53 was depleted in A549 cells, telomerase activity was still blocked by reFIP-gts (Fig. 5A, left panel). When overexpression of p53 was stabilized in H1299 cells, reFIP-gts did not inhibit telomerase activity (Fig. 5A, right panel). Therefore, the reduction in telomerase activity by reFIP-gts is P53 independent.

3.5. Recombinant FIP-gts suppresses telomerase activity in A549 cells but not in H1299 cells via calcium induction

Previous studies have shown that accumulation of wild-type proteins in ER leads to a release of Ca^{2+} from organelles that can be blocked by Ca^{2+} chelators [21]. To further study whether ER stress results in the release of Ca^{2+} from organelles, we analyzed intracellular calcium levels in reFIP-gts-treated cells.

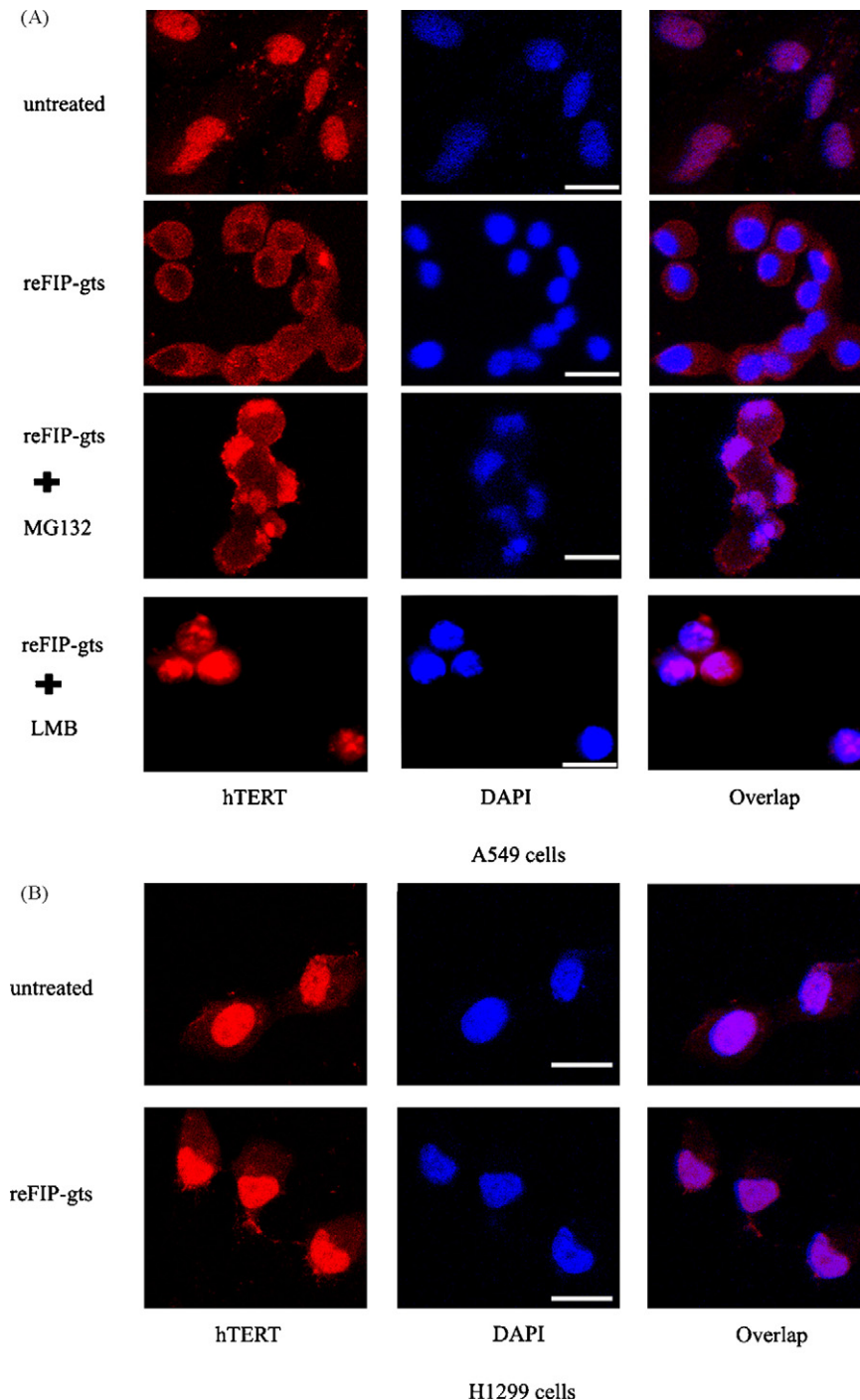


Fig. 7 – Nuclear export of hTERT occurs through nuclear pores and proteasome-mediated manner in A549 cells. (A) Representative immunostaining using confocal microscopy is shown for A549 cell treatment with 1.2 μ M FIP-gts for 48 h. (second panel). A549 cells were co-incubated with 20 μ M of MG132 (third panel) for last 6 h or co-incubated with 20 μ M of Leptomycin B (fourth panel) for last 2 h. hTERT staining (Rhodamine-Red), nuclear staining with DAPI stain (DAPI-Blue). Scale bar indicates 20 μ m. **(B)** Representative immunostaining using confocal microscopy is shown for H1299 cell treatment with 1.2 μ M FIP-gts for 48 h. (second panel). **(C)** In A549 cells, telomerase enzyme activity was measured in the presence or absence of 1.2 μ M FIP-gts (lane 1 and lane 2) or 1.2 μ M FIP-gts and 20 μ M of LMB (lane 2 and lane 3) or 1.2 μ M FIP-gts and MG132 (lane 2 and lane 4). A549 cells were incubated with either leptomycin B or MG132 alone in lane 5 and lane 6. Telomerase activity in each sample was detected on TRAP assay. Internal control, the 36-bp internal standard was used as control. NC: no telomerase extract was added. The data are representative of three independent experiments. **(D)** A549 cells were pretreated with BAPTA-AM for 1 h followed by exposure to reFIP-gts for 48 h. Target protein, phosphorylated Akt ser473 (p-Akt ser473), total Akt (T-Akt) were detected by Western blot. (For interpretation of the references to colour in this figure legend, the reader is referred to the web version of the article.)

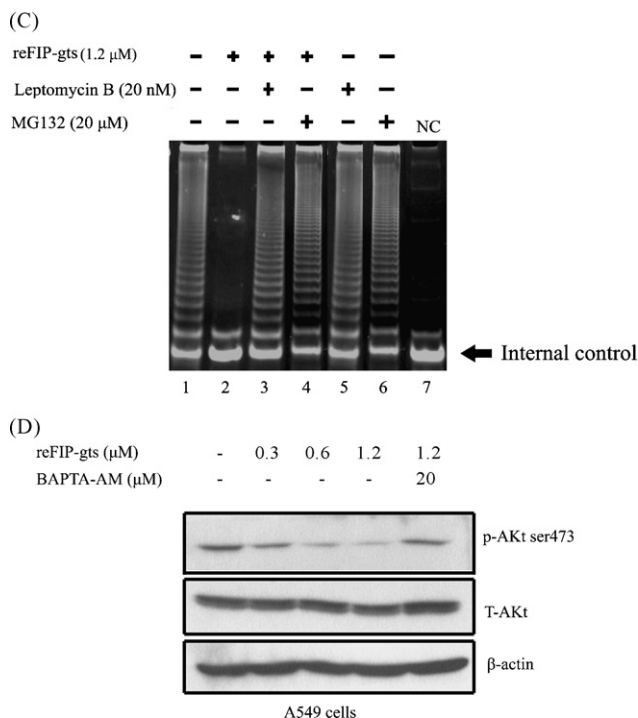


Fig. 7. (Continued).

ER stress induced by thapsigargin is accompanied by release of Ca^{2+} , which can be detected using Fluo-3 calcium indicators. This was evidenced by increased green staining in A549 cells after treatment with thapsigargin for 6 h, in which calcium increased 15-fold (Fig. 6A and C). Following the same staining protocol, we obtained similar results in A549 cells after treatment with 1.2 μ M reFIP-gts for 6 and 24 h, resulting in a 16- and 19-fold induction of calcium, respectively (Fig. 6A and C). Calcium fluorescence only increased 2.5-fold in H1299 cells after treatment with 1.2 μ M reFIP-gts for 24 h (Fig. 6A and C). These results suggest that, like thapsigargin, reFIP-gts induces release of Ca^{2+} from ER and activates ER stress in A549 cells. To confirm specificity for calcium in reFIP-gts-induced-A549 cells, cells were pretreated with calcium chelator BAPTA-AM for 1 h and then with reFIP-gts for 24 h. Analysis of calcium fluorescence revealed a 15-fold induction of calcium following treatment with reFIP-gts alone. When reFIP-gts treatment was combined with BAPTA-AM, the influx of calcium mediated by reFIP-gts was inhibited, resulting in calcium levels similar to those of the untreated sample (Fig. 6B and D). In order to verify the role specificity for Ca^{2+} in telomerase regulation by reFIP-gts, A549 cells were treated with 1.2 μ M reFIP-gts \pm BAPTA-AM for 48 h and assayed for telomerase activity. Similar to the previous results, telomerase activity was blocked by reFIP-gts, and the concomitant addition of 20 μ M BAPTA-AM completely abolished the ability of reFIP-gts to repress telomerase activity (Fig. 6E). Using TRAP and RT-PCR, we found that thapsigargin also inhibited telomerase activity and hTERT mRNA levels in A549 cells (Fig. 6F and G). These results indicate that accumulation of reFIP-gts in ER can cause ER stress and increase intracellular Ca^{2+} level. The increased Ca^{2+} level can reduce telomerase activity directly and indirectly. Taken together, these results suggest that reFIP-gts suppresses

telomerase activity by inducing ER stress and calcium release in A549 cells but not in H1299 cells.

3.6. Recombinant FIP-gts induces nuclear export of hTERT via nuclear pores and proteasomal pathway

Recently, the translocation of TERT has been described as one mechanism for posttranscriptional regulation [13,17]. To investigate the effects of reFIP-gts on localization of hTERT, A549 and H1299 cells were incubated with reFIP-gts (1.2 μ M) for 48 h. reFIP-gts treatment resulted in a profound change, namely hTERT changed from being predominantly nuclear to being predominantly cytoplasmic in A549 cells (Fig. 7A, first and second panel from the upper panel). However, reFIP-gts was not able to induce the translocation of hTERT to cytoplasm in H1299 cells (Fig. 7B, first and second panel from the lower panel).

We then became interested in the underlying mechanism behind the change in A549 cells. The best-characterized inhibitor for CRM1-Ran-dependent transport is leptomycin B [34]. We found that leptomycin B could inhibit reFIP-gts-induced hTERT export into the cytosol (Fig. 7A, fourth panel from the upper panel). Moreover, treatment with leptomycin B restored reFIP-gts-induced inhibition of telomerase enzyme activity (Fig. 7C, lanes 2 and 3).

Proteasome activity and ubiquitination have also been implicated in directing the subcellular localization of many molecules, including HSV-1 UL9 and p53 [35,36]. We investigated whether the loss of nuclear hTERT protein expression and its detection in the cytoplasm was a result of proteasomal-regulated translocation. To do this, we treated A549 cells for 42 h with reFIP-gts and incubated the cells with MG132 for 6 h, to inhibit the chymotrypsin-like activity of the 26S proteasome. Once proteasome activity was inhibited, hTERT was found to accumulate in the nuclei of A549 cells (Fig. 6A, third panel from the upper panel). We also found that by incubating the cells with MG132 we could rescue reFIP-gts-induced suppression of telomerase activity (Fig. 7C, lanes 2 and 4). In the absence of reFIP-gts treatment, incubation of cells with either leptomycin B or MG132 alone did not significantly change the levels of telomerase, when compared with the untreated controls (Fig. 7C, lanes 1, 5 and 6, respectively). These results indicate that reFIP-gts-induced down-regulation of telomerase activity is caused by translocation of telomerase and proteasome-mediated degradation. It has been shown that increased intracellular calcium concentrations can cause a decrease in the phosphorylation of Akt at Ser473 [37]. We found that reFIP-gts may deactivate Akt kinase by preventing phosphorylation of Ser⁴⁷³ residues (Fig. 7D). Similarly, phosphorylated Akt decreased in the presence of reFIP-gts, and the concomitant addition of 20 μ M BAPTA-AM completely restored the ability of reFIP-gts to deactivate p-AKT, suggesting that calcium signal can regulate Akt kinase activity which in turn decreases phosphorylation of hTERT.

4. Discussion

In the present study, reFIP-gts-induced suppression of telomerase activity depended on several factors (Figs. 1B

and 3C, right). Regardless of whether p53 was depleted or over-expressed, reFIP-gts inhibited telomerase activity in A549 cells but not in H1299 cells (Fig. 5), a finding consistent with other studies that have reported that telomerase expression in tumors does not correlate with p53 status [9,33]. reFIP-gts suppressed telomerase activity in A549 cells, but not in H1299 cells, via calcium induction (Fig. 1A, Fig. 3, left and Fig. 6). In addition, reFIP-gts caused different changes in A549 and H1299 cell localization of endogenous hTERT (Fig. 7) and hTERT protein stability (Fig. 4). Taken together, our results show for the first time that reFIP-gts is located in endoplasmic reticulum. It activates a novel pathway for ER stress to induce calcium release and reduce telomerase activity. We also identified a mechanism through which reFIP-gts induces dramatic changes in hTERT localization. Prevention of nuclear export of hTERT with leptomycin B and MG132 significantly enhanced telomerase activity in the presence of reFIP-gts.

In general, *in vitro* fungal immunomodulatory proteins (FIPs) mitogenically stimulate human peripheral blood lymphocytes (hPBLs) and mouse splenocytes via T-cell receptor (TcR) complex [18,19]. To date, little research has been conducted on FIPs ability to prevent cancer. In a previous study, we demonstrated that reFIP-gts inhibited telomerase activity by diminishing the binding capacity of c-Myc for the hTERT promoter [20], and in this study we have shown that reFIP-gts represses c-Myc binding to endogenous hTERT promoter in A549 cells (Fig. 1C). Although FIPs have been found to have immunomodulatory properties, it is not known for sure whether FIPs enter cancer cells to do this. This study used immunofluorescence and confocal microscopy to observe the subcellular localization of reFIP-gts into ER of A549 cells for the first time. However, we could not determine how reFIP-gts enters ER. We will investigate whether reFIP-gts is diffused or endocytosed there in future studies.

We conjectured that the accumulation of reFIP-gts in ER triggers a stress response. Our RT-PCR analysis revealed that reFIP-gts increases mRNA levels of CHOP/GADD153, an indicator of ER stress in A549 cells. Because the ER stores large amounts of Ca^{2+} that can be released upon stimulation, we assumed that the accumulation of proteins in the ER membrane increases its Ca^{2+} permeability. Ca^{2+} has been found to be necessary for thapsigargin-induced ER stress to activate NF- κ B. When Ca^{2+} chelator BAPTA-AM is used to preincubate cells before thapsigargin treatment, ER stress induction of NF- κ B is prevented [38]. In our study, Ca^{2+} chelator BAPTA-AM was found to prevent reFIP-gts suppression of telomerase activity, demonstrating that telomerase is downregulated by reFIP-gts via a Ca^{2+} -dependent pathway. We found that reFIP-gts did not induce GADD153, and calcium release merely increased 2.5-fold in H1299 cells when compared with A549 cells (calcium release increased 19-fold) after treatment with 1.2 μM reFIP-gts for 24 h, suggesting that reFIP-gts was unable to induce ER stress in H1299 cells. Calcium is an intracellular second messenger, which regulates growth arrest and differentiation or apoptotic cell death. An increase in intracellular calcium levels also occurs during differentiation with epidermis exhibiting a calcium gradient increase with differentiation and inhibition of telomerase activity [16]. Consistent with this idea, differentiation and expression of differentiation-specific proteins are strongly

linked with the ability of reFIP-gts to increase intracellular calcium in A549 lung cancer cells.

Recently, the translocation of TERT has been described as the mechanism behind posttranscriptional regulation, and telomerase has been found to shuttle between subcellular compartments during assembly and in response to specific stimuli. TERT is translocated from cytoplasm to the nucleus after activation of T lymphocytes [17] and stimulation of smooth muscle cells by growth factors increases nuclear TERT [39]. These studies suggest that proliferating stimuli increase the activity of nuclear telomerase enzyme, allowing telomere length and subsequently the proliferative capacity of the cells to be maintained. In contrast, oxidative stress has been reported to cause the nuclear export of hTERT by triggering the activation of Ran GTPase and Src kinase family-dependent phosphorylation of Tyrosine707 [40], although we could not detect ROS generation by reFIP-gts (data not shown). We suggest that reFIP-gts-induced translocation of hTERT inhibits telomerase activity via other pathways.

The present study demonstrates that reFIP-gts induces the export of hTERT in A549 cells. Some studies have shown that Ran GTPase may be involved in nuclear transport [13,40]. Recently, the nuclear export receptor CRM1 has been found to bind to TERT [13]. This receptor together with the GTPase Ran can bind large cargo molecules and transport them through the nuclear pores into the cytosol. These findings suggest that reFIP-gts-induced translocation of hTERT from the nucleus into the cytosol may be dependent on the CRM1-Ran-dependent transport pathway. Moreover, pharmacological inhibition of the CRM1-binding capacity to its export cargos with leptomycin B prevents reFIP-gts-induced nuclear export of hTERT. One recent study of telomerase regulation has shown that genistein suppresses telomerase activity through decreased phosphorylation of hTERT, forcing it to translocate from the nucleus to the cytoplasm [41]. Furthermore, previous studies have reported that 14-3-3 proteins, NF- κ B p65, nucleolin and Akt are posttranslational modifiers of telomerase, which is involved in the intracellular localization of hTERT [13,14,41,42]. The difference in translocation of hTERT in A549 and H1299 cells in response to reFIP-gts may be related to these factors. Further studies will be necessary to identify the precise molecular mechanism behind the differential translocation response to reFIP-gts in A549 and H1299 cells.

In addition, ubiquitination is the predominant mechanism behind the destruction of protein. Conjugation of proteins to ubiquitin can influence their cellular localization [43]. The G-quadruplex-interactive molecule BRACO-19 has been reported to interfere with telomerase function and to decrease the expression of hTERT in the nucleus via ubiquitin for subsequent destruction in the proteasome [44]. When we co-incubated A549 cells with MG132 and reFIP-gts, 26S proteasome activity was inhibited and telomerase function was restored. Proteasome plays an important role in repressing telomerase activity by reFIP-gts and is involved in maintaining a dynamic balance between exporting and importing, which affects the stability of hTERT.

There are fundamental differences between A549 and H1299 cell lines other than in P53 status. These include differences in uptake of reFIP-gts resulting in differences in histologic subtype, specifically adenocarcinoma and large cell

carcinoma for A549 and H1299 cell lines, respectively. We presumed that reFIP-gts causes ER stress induction and calcium release in A549 cells, but not in H1299 cells, through TcR-like complex. In future studies, we will indicate whether other cellular receptors mediate the effects of reFIP-gts in A549 cells.

Based on these findings, the posttranslational modifications of hTERT protein are more important than downregulation of hTERT transcriptional activity in reFIP-gts-induced suppression of telomerase activity in lung cancer cells. Although telomerase activity and hTERT mRNA expression are important prognostic factors in lung cancer patients [45], eradication of telomerase activity is essential in cancer therapy. These new findings may provide useful information for the development of a specific therapeutic strategy for cancer that involves control of telomerase activity.

Acknowledgments

This study was supported by the Committee on Chinese Medicine and Pharmacy, Department of Health, Executive Yuan, ROC (CCMP93-RD-009), Veterans General Hospital-Taichung, Taichung, (TCVGH-964705D) and National Science Council, Taiwan, ROC (NSC 94-2311-B040-003 and NSC 96-2314-B-040-014-MY3).

REFERENCES

- [1] Harley CB, Futcher AB, Greider CW. Telomeres shorten during ageing of human fibroblasts. *Nature* 1990;345:458–60.
- [2] Counter CM, Avilion AA, LeFeuvre CE, Stewart NG, Greider CW, Harley CB, et al. Telomere shortening associated with chromosome instability is arrested in immortal cells which express telomerase activity. *EMBO J* 1992;11:1921–9.
- [3] Wu TC, Lin P, Hsu CP, Huang YJ, Chen CY, Chung WC, et al. Loss of telomerase activity may be a potential favorable prognostic marker in lung carcinomas. *Lung Cancer* 2003;41:163–9.
- [4] Lingner J, Hughes TR, Shevchenko A, Mann M, Lundblad V, Cech TR. Reverse transcriptase motifs in the catalytic subunit of telomerase. *Science* 1997;276:561–7.
- [5] Kyo S, Kanaya T, Takakura M, Tanaka M, Inoue M. Human telomerase reverse transcriptase as a critical determinant of telomerase activity in normal and malignant endometrial tissues. *Int J Cancer* 1999;80:60–3.
- [6] Nakano K, Watney E, McDougall JK. Telomerase activity and expression of telomerase RNA component and telomerase catalytic subunit gene in cervical cancer. *Am J Pathol* 1998;153:857–64.
- [7] Fujita Y, Fujikane T, Fujiuchi S, Nishigaki Y, Yamazaki Y, Nagase A, et al. The diagnostic and prognostic relevance of human telomerase reverse transcriptase mRNA expression detected in situ in patients with nonsmall cell lung carcinoma. *Cancer* 2003;98:1008–13.
- [8] Ducrest AL, Szutorisz H, Lingner J, Nabholz M. Regulation of the human telomerase reverse transcriptase gene. *Oncogene* 2002;21:541–52.
- [9] Lin SY, Elledge SJ. Multiple tumor suppressor pathways negatively regulate telomerase. *Cell* 2003;113:881–9.
- [10] Wu KJ, Grandori C, Amacker M, Simon-Vermot N, Polack A, Lingner J, et al. Direct activation of TERT transcription by c-MYC. *Nat Genet* 1999;21:220–4.
- [11] Kang SS, Kwon T, Kwon DY, Do SI. Akt protein kinase enhances human telomerase activity through phosphorylation of telomerase reverse transcriptase subunit. *J Biol Chem* 1999;274:13085–90.
- [12] Xu D, Wang Q, Gruber A, Bjorkholm M, Chen Z, Zaid A, et al. Downregulation of telomerase reverse transcriptase mRNA expression by wild type p53 in human tumor cells. *Oncogene* 2000;19:5123–33.
- [13] Seimiya H, Sawada H, Muramatsu Y, Shimizu M, Ohko K, Yamane K, et al. Involvement of 14-3-3 proteins in nuclear localization of telomerase. *EMBO J* 2000;19:2652–61.
- [14] Akiyama M, Hideshima T, Hayashi T, Tai YT, Mitsiades CS, Mitsiades N, et al. Nuclear factor-kappaB p65 mediates tumor necrosis factor alpha-induced nuclear translocation of telomerase reverse transcriptase protein. *Cancer Res* 2003;63:18–21.
- [15] Holt SE, Wright WE, Shay JW. Regulation of telomerase activity in immortal cell lines. *Mol Cell Biol* 1996;16:2932–9.
- [16] Rosenberger S, Thorey IS, Werner S, Boukamp P. A novel regulator of telomerase. S100A8 mediates differentiation-dependent and calcium-induced inhibition of telomerase activity in the human epidermal keratinocyte line HaCaT. *J Biol Chem* 2007;282:6126–35.
- [17] Liu K, Hodes RJ, Weng N. Cutting edge: telomerase activation in human T lymphocytes does not require increase in telomerase reverse transcriptase (hTERT) protein but is associated with hTERT phosphorylation and nuclear translocation. *J Immunol* 2001;166:4826–30.
- [18] Ko JL, Hsu CI, Lin RH, Kao CL, Lin JY. A new fungal immunomodulatory protein, FIP-fve isolated from the edible mushroom, *Flammulina velutipes* and its complete amino acid sequence. *Eur J Biochem* 1995;228:244–9.
- [19] Wang PH, Hsu CI, Tang SC, Huang YL, Lin JY, Ko JL. Fungal immunomodulatory protein from *Flammulina velutipes* induces interferon-gamma production through p38 mitogen-activated protein kinase signaling pathway. *J Agric Food Chem* 2004;52:2721–5.
- [20] Liao CH, Hsiao YM, Hsu CP, Lin MY, Wang JC, Huang YL, et al. Transcriptionally mediated inhibition of telomerase of fungal immunomodulatory protein from *Ganoderma tsugae* in A549 human lung adenocarcinoma cell line. *Mol Carcinog* 2006;45:220–9.
- [21] Pahl HL. Signal transduction from the endoplasmic reticulum to the cell nucleus. *Physiol Rev* 1999;79:683–701.
- [22] Ellgaard L, Helenius A. Quality control in the endoplasmic reticulum. *Nat Rev Mol Cell Biol* 2003;4:181–91.
- [23] Thastrup O, Cullen PJ, Drobak BK, Hanley MR, Dawson AP, Thapsigargin. a tumor promoter, discharges intracellular Ca^{2+} stores by specific inhibition of the endoplasmic reticulum Ca^{2+} -ATPase. *Proc Natl Acad Sci USA* 1990;87:2466–70.
- [24] Lytton J, Westlin M, Hanley MR. Thapsigargin inhibits the sarcoplasmic or endoplasmic reticulum Ca -ATPase family of calcium pumps. *J Biol Chem* 1991;266:17067–71.
- [25] Bickenbach JR, Vormwald-Dogan V, Bacher C, Bleuel K, Schnapp G, Boukamp P. Telomerase is not an epidermal stem cell marker and is downregulated by calcium. *J Invest Dermatol* 1998;111:1045–52.
- [26] Alfonso-De Matte MY, Kruk PA. Phosphatidylinositol triphosphate kinase-dependent and c-jun NH2-terminal kinase-dependent induction of telomerase by calcium requires Pyk2. *Cancer Res* 2004;64:23–6.
- [27] Ko JL, Chiao MC, Chang SL, Lin P, Lin JC, Sheu GT, et al. A novel p53 mutant retained functional activity in lung carcinomas. *DNA Repair (Amst)* 2002;1:755–62.

- [28] Nawrocki ST, Carew JS, Dunner Jr K, Boise LH, Chiao PJ, Huang P, et al. Bortezomib inhibits PKR-like endoplasmic reticulum (ER) kinase and induces apoptosis via ER stress in human pancreatic cancer cells. *Cancer Res* 2005;65:11510–9.
- [29] Orlando V, Strutt H, Paro R. Analysis of chromatin structure by in vivo formaldehyde cross-linking. *Methods* 1997;11:205–14.
- [30] Wu YL, Dudognon C, Nguyen E, Hillion J, Pendino F, Tarkanyi I, et al. Immunodetection of human telomerase reverse-transcriptase (hTERT) re-appraised: nucleolin and telomerase cross paths. *J Cell Sci* 2006;119:2797–806.
- [31] Kaufman RJ. Orchestrating the unfolded protein response in health and disease. *J Clin Invest* 2002;110:1389–98.
- [32] Kanaya T, Kyo S, Hamada K, Takakura M, Kitagawa Y, Harada H, et al. Adenoviral expression of p53 represses telomerase activity through down-regulation of human telomerase reverse transcriptase transcription. *Clin Cancer Res* 2000;6:1239–47.
- [33] Sood AK, Coffin J, Jabbari S, Buller RE, Hendrix MJ, Klingelhutz A. p53 null mutations are associated with a telomerase negative phenotype in ovarian carcinoma. *Cancer Biol Ther* 2002;1:511–7.
- [34] Kudo N, Matsumori N, Taoka H, Fujiwara D, Schreiner EP, Wolff B, et al. Leptomycin B inactivates CRM1/exportin 1 by covalent modification at a cysteine residue in the central conserved region. *Proc Natl Acad Sci USA* 1999;96:9112–7.
- [35] Lee DH, Goldberg AL. Proteasome inhibitors: valuable new tools for cell biologists. *Trends Cell Biol* 1998;8:397–403.
- [36] Kisselev AF, Goldberg AL. Proteasome inhibitors: from research tools to drug candidates. *Chem Biol* 2001;8:739–58.
- [37] King TD, Gandy JC, Bijur GN. The protein phosphatase-1/inhibitor-2 complex differentially regulates GSK3 dephosphorylation and increases sarcoplasmic/endoplasmic reticulum calcium ATPase 2 levels. *Exp Cell Res* 2006;312:3693–700.
- [38] Pahl HL, Baeuerle PA. Activation of NF-kappa B by ER stress requires both Ca²⁺ and reactive oxygen intermediates as messengers. *FEBS Lett* 1996;392:129–36.
- [39] Minamino T, Kourembanas S. Mechanisms of telomerase induction during vascular smooth muscle cell proliferation. *Circ Res* 2001;89:237–43.
- [40] Haendeler J, Hoffmann J, Brandes RP, Zeiher AM, Dimmeler S. Hydrogen peroxide triggers nuclear export of telomerase reverse transcriptase via Src kinase family-dependent phosphorylation of tyrosine 707. *Mol Cell Biol* 2003;23:4598–610.
- [41] Jagadeesh S, Kyo S, Banerjee PP. Genistein represses telomerase activity via both transcriptional and posttranslational mechanisms in human prostate cancer cells. *Cancer Res* 2006;66:2107–15.
- [42] Khurts S, Masutomi K, Delgermaa L, Arai K, Oishi N, Mizuno H, et al. Nucleolin interacts with telomerase. *J Biol Chem* 2004;279:51508–15.
- [43] Weissman AM. Themes and variations on ubiquitylation. *Nat Rev Mol Cell Biol* 2001;2:169–78.
- [44] Burger AM, Dai F, Schultes CM, Reszka AP, Moore MJ, Double JA, et al. The G-quadruplex-interactive molecule BRACO-19 inhibits tumor growth, consistent with telomere targeting and interference with telomerase function. *Cancer Res* 2005;65:1489–96.
- [45] Zhu CQ, Cutz JC, Liu N, Lau D, Shepherd FA, Squire JA, et al. Amplification of telomerase (hTERT) gene is a poor prognostic marker in non-small-cell lung cancer. *Br J Cancer* 2006;94:1452–9.